Cerebral Circulation - Cognition and Behavior 6 (2024) 100203

Contents lists available at ScienceDirect

Cerebral Circulation - Cognition and Behavior

journal homepage: www.sciencedirect.com/journal/cerebral-circulation-cognition-and-behavior

Correlates of axonal content in healthy adult span: Age, sex, myelin, and metabolic health

Agnieszka Z Burzynska [a,#,*], Charles Anderson [b], David B. Arciniegas [c], Vince Calhoun [d], In-Young Choi [e], Andrea Mendez Colmenares [a], Arthur F Kramer [f,k], Kaigang Li [g], Jongho Lee [h], Phil Lee [i], Michael L Thomas [j]

[a] The BRAiN lab, Department of Human Development and Family Studies/Molecular, Cellular and Integrative Neurosciences, Colorado State University, Fort Collins, CO, USA
[b] Department of Computer Science, Colorado State University, Fort Collins, CO, USA
[c] Marcus Institute for Brain Health, University of Colorado Anschutz Medical Campus, Aurora, CO, USA
[d] Tri-institutional Center for Translational Research in Neuroimaging and Data Science (TReNDS), Georgia State, Georgia Tech, Emory, Atlanta, GA, USA
[e] Department of Neurology, Department of Radiology, Hoglund Biomedical Imaging Center, University of Kansas Medical Center, Kansas City, KS, USA
[f] Beckman Institute for Advanced Science and Technology at the University of Illinois, IL, USA,
[g] Department of Health and Exercise Science, Colorado State University, Fort Collins, CO, USA
[h] Department of Electrical and Computer Engineering, Seoul National University, Seoul, Republic of Korea
[i] Department of Radiology, Hoglund Biomedical Imaging Center, University of Kansas Medical Center, Kansas City, KS, USA
[j] Department of Psychology, Colorado State University, Fort Collins, CO, USA
[k] Center for Cognitive & Brain Health, Northeastern University, Boston, MA, USA

ARTICLE INFO

Keywords:
Axons
White matter
Aging
Myelin
Metabolic syndrome
Obesity
Adiposity
BMI

ABSTRACT

As the emerging treatments that target grey matter pathology in Alzheimer's Disease have limited effectiveness, there is a critical need to identify new neural targets for treatments. White matter's (WM) metabolic vulnerability makes it a promising candidate for new interventions. This study examined the age and sex differences in estimates of axonal content, as well the associations of with highly prevalent modifiable health risk factors such as metabolic syndrome and adiposity. We estimated intra-axonal volume fraction (ICVF) using the Neurite Orientation Dispersion and Density Imaging (NODDI) in a sample of 89 cognitively and neurologically healthy adults (20–79 years). We showed that ICVF correlated positively with age and estimates of myelin content. The ICVF was also lower in women than men, across all ages, which difference was accounted for by intracranial volume. Finally, we found no association of metabolic risk or adiposity scores with the current estimates of ICVF. In addition, the previously observed adiposity-myelin associations (Burzynska et al., 2023) were independent of ICVF. Although our findings confirm the vulnerability of axons to aging, they suggest that metabolic dysfunction may selectively affect myelin content, at least in cognitively and neurologically healthy adults with low metabolic risk, and when using the specific MRI techniques. Future studies need to revisit our findings using larger samples and different MRI approaches, and identify modifiable factors that accelerate axonal deterioration as well as mechanisms linking peripheral metabolism with the health of myelin.

Introduction

Treatments that target grey matter pathology in Alzheimer's Disease (AD) have only limited effectiveness in slowing dementia progression and are thought to be the most effective in the early stages of the disease [1]. Therefore, there is a critical need to identify new neural targets for future treatments, early disease biomarkers, as well as protective factors that may help postpone AD and decelerate brain aging.

We argue that the white matter (WM), containing mostly myelinated axons, may be the overlooked neural target and early biomarker of AD.

* Corresponding author at: Department of Human Development and Family Studies, Molecular, Cellular and Integrative Neurosciences, Colorado State University, Campus Delivery 1570, Fort Collins, CO 80523-1570, USA.
E-mail address: agaburza@colostate.edu (A.Z. Burzynska).
Except the first author, all other authors are listed in A to Z order.

https://doi.org/10.1016/j.cccb.2024.100203
Received 23 October 2023; Received in revised form 10 January 2024; Accepted 11 January 2024
Available online 12 January 2024

Mounting histopathological evidence suggests that AD pathology in the grey matter (i.e., amyloid and tau deposits) is not only accompanied, but often preceded by WM pathology, such as defects in axonal structure and transportation, and failed myelin repair [2–4]. With myelin often in the spotlight, less is known about the role of axons in cognitive decline, possibly due to the methodological limitations of the most commonly used method, diffusion tensor imaging (DTI). Diffusion is modulated by multiple tissue properties, such as axonal diameter and density, myelin content, fiber orientational coherence, extracellular water, as well as other glia. As the DTI model represents the diffusion of water protons in the tissue as a single ellipsoid, the resulting metrics – such as fractional anisotropy or mean diffusivity – provide only limited information about the content or integrity of axons or myelin [5]. Therefore, more advanced diffusion models are needed to disentangle axonal orientation from intra- and extra-cellular diffusion.

To address this gap, in the current study, we used a more advanced model for diffusion of WM tissue, Neurite Orientation Dispersion and Density Imaging (NODDI), to estimate axonal content. NODDI combines a multi-shell high-angular-resolution diffusion imaging with three-compartment tissue modelling (intra-, extra-cellular and cerebrospinal fluid; [6,7]) to yield separate, voxel-wise estimation of 1) intra-cellular volume fraction (ICVF) reflecting axonal content, 2) orientation dispersion index of the fibers, and 3) extracellular isotropic volume fraction, reflecting extracellular cerebrospinal fluid [7].

The existing studies using NODDI reported mixed findings regarding age differences in axonal content estimated as ICVF. Some reported linear or quadratic declines, whereas others reported increases in ICVF, or no associations with age [8–20]. This may be because only few of these samples spanned the entire adulthood [8,10,12,18,19], which is necessary to capture quadratic or inverted U-shaped functions of ICVF with age. For example, samples weighted more heavily on young to middle-aged adults may detect only the increase in ICVF and fail to detect the subsequent peak and a decrease (e.g., [11,14,20]), whereas samples with only middle-aged to older participants (e.g., [13]) may capture primarily linear declines. The differences in previous findings could also stem from differences in inclusion/exclusion criteria, acquisition, preprocessing, and modelling of NODDI images, as well as statistical power and sample size (e.g., $n = 47$ in Kodiweera et al., [14] vs. $n = 3513$ in [13]). Furthermore, few studies investigated sex differences [8,12,15,17–19] or relationships of myelin with axonal content [11,21,18] yielding inconsistent results.

Most importantly, health risk factors for axonal health are unknown. Maintenance of the axonal structure and the long-distance cellular transport is prone to oxidative stress, vascular insults, inflammation, and metabolic dysfunction. These not only accumulate with age and in neurodegenerative diseases [3], but are also amplified by common health conditions related to metabolic syndrome (MetS; [22,23]). MetS components include excess abdominal fat (visceral adiposity), elevated fasting blood glucose, elevated blood pressure (BP), abnormal blood cholesterol, and elevated triglyceride levels [24]. Two earlier studies reported a negative association of measures of adiposity and quantitative MRI estimates of myelin. First, body mass index (BMI) and waist circumference (WC) negatively correlated with myelin water fraction in healthy adults of age 22 to 94 [12]. Second, greater BMI was correlated with significantly lower R1 (1/T1-weighted signal) in young lean, overweight, and obese adults, attributed to decreased myelin [25]. Recently, we extended these findings by showing that MetS risk score (comprising of BMI, WC, BP and history of dyslipidemia and hyperglycemia), as well as adiposity sub-score (combined BMI and WC) correlated with lower myelin water fraction in healthy adults of age 20–79 [26]. However, whether axons are affected by MetS risk or adiposity in a similar way is unknown.

Taken together, the aim of the current study was to investigate the age- and sex-related differences in estimates of axonal content, the regional axon-myelin associations, and the associations of MetS risk score and adiposity sub-score with axonal content in a healthy adult-span sample. Given the trophic support that oligodendrocytes provide to axons [27], we expected to observe a positive association between myelin and axonal content and a negative association of MetS risk and adiposity scores with ICVF, particularly in the late-myelinating, more vulnerable WM regions.

Methods

Core methods for the current study are provided in our previously published work Burzynska et al. [26]. Here we report only information that is unique or directly relates to the current analyses. All other details are available in Appendix A.

Participants

The study was approved by the Colorado State University Institutional Review Board.

Inclusion criteria included the ability to give informed consent and age 20–80 years. Exclusion criteria were designed to define homogenous and neurologically, psychiatrically, and cognitively healthy adult sample, as defined previously for the Human Connectome Project in Aging (HCP-A; [28]). In addition, we used the following exclusion criteria: <30 score on modified Telephone Interview of Cognitive Status (TICS-M) questionnaire [29], one or more standard deviations below age- and education-based performance on Mini-Mental State Examination (MMSE; [30,31]), >0 on Clinical Dementia Rating (CDR; [32]), >10 on the short form of Geriatric Depression Scale (GDS-15; [33]), <9 years of education, smoking>20 cigarettes or joints/month, mean resting systolic blood pressure >140 [34], body mass index (BMI) >33 [35,36], and >2 on the modified Hachinski ischemic scale [37].

See Appendix B for the subject flow. The current sample differs from the previous study by one participant, whose NODDI data is missing due to a technical problem.

MRI acquisition

Imaging was performed on a 3T MRI system (Siemens MAGNETOM Skyra, Erlangen, Germany) with a 64-channel RF coil. The acquisition parameters used in this study are the following: Diffusion-weighted images were acquired using a multi-shell (b = 0,1000, 2000s/mm^2) high-angular-resolution (138 directions) multiband echo planar sequence in transversal plane (TE/TR = 104.8/3120 ms, FOV = 234 mm, resolution = 1.8 mm^3, 76 slices, multiband acceleration factor = 4, flip angle 79°, refocus flip angle 160°). The scan was repeated for both anterior-to-posterior and posterior-to-anterior phase encoding directions, each lasting 7.31 min. For details on myelin water imaging (MWI) see Appendix A and Burzynska et al. [26].

Image analysis and registration

From the pairs of the DWIs acquired with reversed phase-encoding blips, susceptibility-induced off-resonance field was estimated [38], as implemented in FSL as *topup* [39], generating a single corrected (or unwarped) b = 0 image. Then, the *topup* distortion correction was applied using *eddy* in FSL [40], which also corrected for distortions related to eddy current and motion. The diffusion tensor model was fitted to the data using the FSL Diffusion Toolbox v.5.0 (FDT), yielding the fractional anisotropy (FA) maps, whereas the NODDI modelling was performed using Matlab toolbox v. 1.05. (https://www.nitrc.org/projects/noddi_toolbox/) which generated maps of the volume fraction of intra-axonal compartment (i.e., intra-cellular volume fraction; ICVF), as well as volume fraction of Gaussian isotropic diffusion compartment, representing extracellular free water (cerebrospinal fluid), and orientational dispersion index of the axons. In the current study, only ICVF analyses were used. ICVF values range from 0 to 1, where 0.07, for example, reflects 7 % axonal volume fraction, and 0.65 reflects 65 %

axonal volume fraction.

Then, we used the tract-based spatial statistics (TBSS; [41]) workflow in FSL v6.0.5.2 to skeletonize the FA values. Then, we applied tbss_non_FA procedure to ICVF maps aligned with the unwarped $b = 0$ images to project the ICVF values on the skeleton from the same voxels as for MWF in the previous study (Burzynska et al. [26] for the image processing illustration and Appendix A for more details on MWF analysis). All steps of image processing as well as registrations for all participants were visually inspected in either FSLeyes or by using slicesdir command. The *eddy*- and *topup*-corrected, brain-extracted b0 images were used to estimate intracranial volume (voxel number × voxel size, in mm^3), which was used for analyses of sex differences.

Regions of interest

To estimate ICVF in the entire WM, we averaged the ICVF values from the entire skeleton for each participant (whole WM). Next, we extracted mean ICVF values from regions (Table 1) representing the major association, projection, and commissural fibers, as described recently [26]. Specifically, the 14 regions included the genu, body and splenium of the corpus callosum, prefrontal WM, cingulum, corticospinal tract, uncinate, fornix, superior longitudinal fasciculus, external capsule, anterior limb of the internal capsule, and the WM of the medial prefrontal cortex and the temporal lobe. Mean ICVF was extracted from each region using *fslmeants* in FSL.

Metabolic syndrome and adiposity scores

We collected ambulatory blood pressure (BP), waist circumference (WC), weight, height, and the derived BMI, as well as self-reported information on history of cholesterolemia and hyperglycemia (see [26], and Appendix A for details). The "MetS risk score" was computed by adding the z-scored values of mean systolic BP, WC, BMI, and self-reports history of elevated cholesterol and sugar. The "adiposity sub-score" was estimated by adding the z-scored values of BMI and WC as described earlier [26,42].

In addition, to provide comparison with MetS population statistics, we created a proxy for MetS diagnosis, following the guidelines by the International Diabetes Federation [24]. Namely, each participant received "1" if they had a history of dyslipidemia, hyperglycemia, systolic BP >130 or diastolic BP >85, and if their WC was in the range of overweight or obese for their sex. Thus, the possible scored ranged from 0 to 4, where score of 3 or 4 indicated possible MetS diagnosis and score of 2 possible pre-MetS. We use the term "possible" as our data on dyslipidemia and blood glucose were based on self-report.

Statistical analyses

Bivariate Pearson's correlations were used to assess the linear and quadratic (age^2 =age × age) effects of age on ICVF. The inclusion of age^2 as an independent variable is based on others' recent observations that ICVF follows a quadratic relationship with age [8,10,13,18]. As these results are reported for future meta-analyses, Table 2 includes raw p-values (not corrected for multiple comparisons). Effect sizes were as considered small ($0.2 \leq r < 0.3$), medium ($0.3 \leq r < 0.5$) or large ($r \geq 0.5$) for both correlations and standardized β coefficients in regressions [43]. Next, to test the hypothesis that ICVF is associated with MetS risk score, we conducted 14 linear regressions, with regional ICVF as the dependent variable, and age, age^2, sex, race, ethnicity, education, income, and MetS risk score as independent variables. In the regression models, to remove nonessential collinearity between age and age^2, the age variable was centered by subtracting the group mean from each individual value, and age^2 was calculated from this centered variable. Similarly, to test whether adiposity is associated with ICVF, we conducted 14 linear regressions, with regional ICVF as the dependent variable, and age, age^2, sex, race, ethnicity, education, income, and adiposity score as independent variables. To test whether controlling for intracranial volume accounts for the sex differences in ICVF, we carried out stepwise linear regressions, where ICVF from regions showing sex differences was the

Table 1
Descriptive Statistics.

	Min	Max	M	SD
Age (years)	20.0	79.0	52.7	17.8
MMSE	27.0	30.0	29.4	0.7
Education (years)	11.0	22.0	17.0	2.6
Income ($/year)	1=<30,000	6=>120,000	>120,000*	1.7
Systolic BP	96.0	151.0	121.0	12.4
WC (cm)	70.0	122.0	94.6	11.3
Height (m)	1.52	1.91	1.678	0.1
Weight (kg)	48.0	110.0	71.5	12.5
BMI	19.0	32.7	25.4	3.5
MetS score	−6.0	6.5	−0.02	3.2
Adiposity score	−4.0	4.03	−0.02	1.8
ICVF				
Whole WM	0.52	0.65	0.60	0.02
Prefrontal	0.47	0.66	0.58	0.03
mPFC	0.39	0.66	0.54	0.05
EC	0.47	0.64	0.56	0.03
SLF	0.58	0.74	0.68	0.03
Genu CC	0.55	0.77	0.67	0.04
Body CC	0.65	0.81	0.74	0.03
Splenium CC	0.69	0.84	0.77	0.03
FX	0.49	0.80	0.62	0.06
TEMP	0.44	0.61	0.53	0.03
ALIC	0.65	0.79	0.71	0.03
UNC	0.44	0.62	0.54	0.03
CING	0.50	0.67	0.59	0.03
CST	0.68	0.79	0.74	0.02

Note: $N = 89$ for all variables. MMSE: mini-mental state examination, BP: blood pressure, WC: waist circumference, BMI: body mass index, ICVF: Intra-cellular volume fraction, WM: white matter, CC: corpus callosum, external capsule (EC), fornix (FX), superior longitudinal fasciculus (SLF), anterior limb of the internal capsule (ALIC), cingulum bundle (CING), uncinate fasciculus (UNC), WM of the medial PFC (mPFC), WM of the temporal pole related to inferior longitudinal fasciculus (TEMP), and corticospinal tract (CST).*Median/mode.

Table 2
Linear and quadratic Pearson's correlations of ICVF with age.

WM region (ICVF)		Age	Age^2
Whole WM	*r*	−0.22	−0.28
	p	0.039	0.009
Prefrontal	*r*	−0.44	−0.48
	p	<0.001	<0.001
mPFC	*r*	−0.48	−0.51
	p	<0.001	<0.001
EC	*r*	−0.15	−0.21
	p	0.170	0.048
SLF	*r*	−0.37	−0.41
	p	<0.001	<0.001
Genu CC	*r*	−0.60	−0.60
	p	<0.001	<0.001
Body CC	*r*	−0.13	−0.13
	p	0.224	0.210
Splenium CC	*r*	−0.07	−0.09
	p	0.536	0.402
FX	*r*	0.49	0.48
	p	<0.001	<0.001
TEMP	*r*	−0.22	−0.27
	p	0.038	0.010
ALIC	*r*	0.08	0.02
	p	0.486	0.892
UNC	*r*	−0.39	−0.44
	p	<0.001	<0.001
CING	*r*	−0.12	−0.17
	p	0.250	0.112
CST	*r*	0.20	0.14
	p	0.060	0.184

Note: All correlations were on $N = 89$; see Table 1 for other abbreviations. P-values are uncorrected.

dependent variable (cingulate, uncinate, corticospinal tract, fornix, external capsule, splenium CC, whole WM, and prefrontal WM), the intracranial volume estimate was entered in the first step, and sex in the second step using the "Enter" method. All analyses were conducted in SPSS v.28. and FDR correction was applied using the Benjamini-Hochberg method, when appropriate. FDR-corrected p-values of 0.05 or smaller were considered significant.

Results

Sample characteristics

Our final sample consisted of 89 neurologically and psychiatrically healthy participants of age 20–79 (25 % men), with MMSE scores indicating no cognitive impairment, as well as BMI and systolic BP values representative of healthy adult population (see Table 1). Although women were over-represented in our sample, this was consistent across all age decades: age 20–29 (n = 18, 15 women), age 30–39 (n = 5, 2 women), age 40–49 (n = 11, 8 women), age 50–59(n = 16, 13 women), age 60–69 (n = 23, 18 women), age 70–79 (n = 16, 11 women). Twenty participants (22.5 %) had a score of three or four according to the International Diabetes Federation [24], suggesting a possible MetS diagnosis. Twenty-eight (31.4 %) had a score of two, suggesting a pre-MetS, and 41 participants (46.1 %) had the score of 0 or 1. MetS risk scores and adiposity sub-scores used for subsequent analyses were continuous variables (Table 1).

Axonal content: age, sex, and intracranial volume

First, we investigated the associations of axonal content (ICVF) with age, and sex, and intracranial volume. Table 1 reports sample characteristics and mean ICVF values for each WM region. Mean ICVF was the highest the splenium CC (77 %), corticospinal tract (74 %), body CC (74 %), and ALIC (71 %), and the lowest in temporal WM (53 %), mPFC and UNC (53 %), and external capsule (56 %). We observed a gradient of ICVF in the corpus callosum, with lowest ICVF in the genu (67 %), intermediate in the body (74 %) and highest in the splenium (77 %).

Table 2 shows region-specific linear and quadratic correlations of ICVF with age. The strongest negative associations (of large effect size, r>=|−0.60|) were observed in the genu CC, followed by medium effect size correlations (r>=|−0.40|) in the prefrontal WM, mPFC WM, UNC, and SLF, and small effect size correlation were in observed in the whole WM and the EC. In regions showing predominantly quadratic associations (i.e., the whole WM, prefrontal WM, EC, UNC), ICVF showed an increase in the age range 20–40, followed by a peak in the 5th decade of life and a subsequent decline. In the genu CC, SLF, and mPFC we observed a linear decrease in ICVF (Fig. 1, see also plots in the Appendix C).

We observed no significant associations in the body and splenium CC, ALIC, cingulum, and corticospinal tract. Only ICVF in the fornix showed both linear and quadratic positive associations with age. Together, our findings support using both age and age^2 as covariates in the subsequent regression models. Fig. 2 shows whole-brain ICVF maps, averaged within each decade of life.

Appendix C contains the results of the two-way ANOVA analyzing the main effects of sex, a decade of life, and sex × decade interaction, as well as the descriptive statistics for ICVF values broken down by sex and age decade, as a reference for future meta-analyses and comparative studies. In brief, we observed the overall main effect of age (p<0.001) on ICVF in the genu cc (p<0.001), uncinate (p<0.001), prefrontal WM (p = 0.001), mPFC WM (p = 0.004), SLF (p = 0.013), EC (p = 0.037), and fornix (p = 0.006), consistent with the correlations reported above.

We found an overall significant effect of sex (p = 0.015), where ICVF was greater in men than women in the cingulate (p = 0.008), uncinate (p = 0.006), corticospinal tract (p = 0.007), fornix (p<0.001), external capsule (p = 0.013), splenium CC (p = 0.005), whole WM (p = 0.026) and prefrontal WM (p = 0.023) (Appendix C). We observed no sex * decade interactions.

Next, investigated the effects of intercranial volume. As expected, men (M=1,725,621 mm^3) had greater intercranial volume than women (M=1,530,024 mm^3) (t=6.78, p<0.001). The intracranial volume was also positively correlated with ICVF in the majority of the studied regions (Table 3). For example, the strongest associations were in the splenium CC, uncinate and cingulate, whereas ALIC, genu and body CC showed no associations. Finally, we checked whether the intracranial volume accounts for the effects of sex on ICVF. Using stepwise linear regression, we found that sex no longer was a significant predictor of ICVF after controlling for intracranial volume (all p-values for sex >0.050).

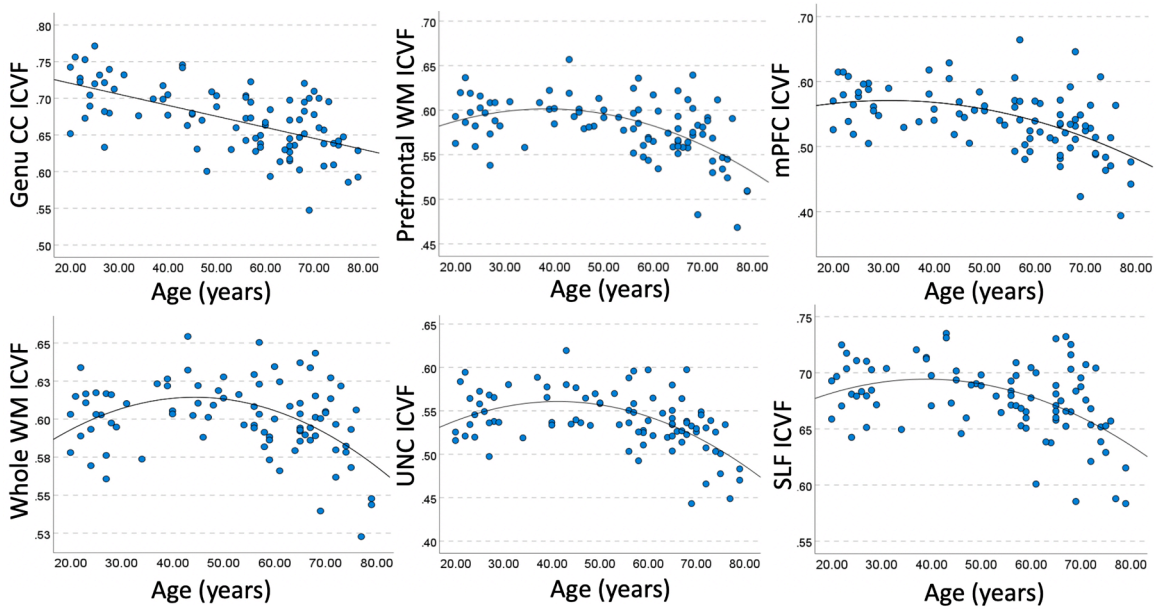

Fig. 1. Example bivariate correlations of age with ICVF. Linear or quadratic fit is shown, depending on the correlation results in Table 2. For abbreviations, see Table 1.

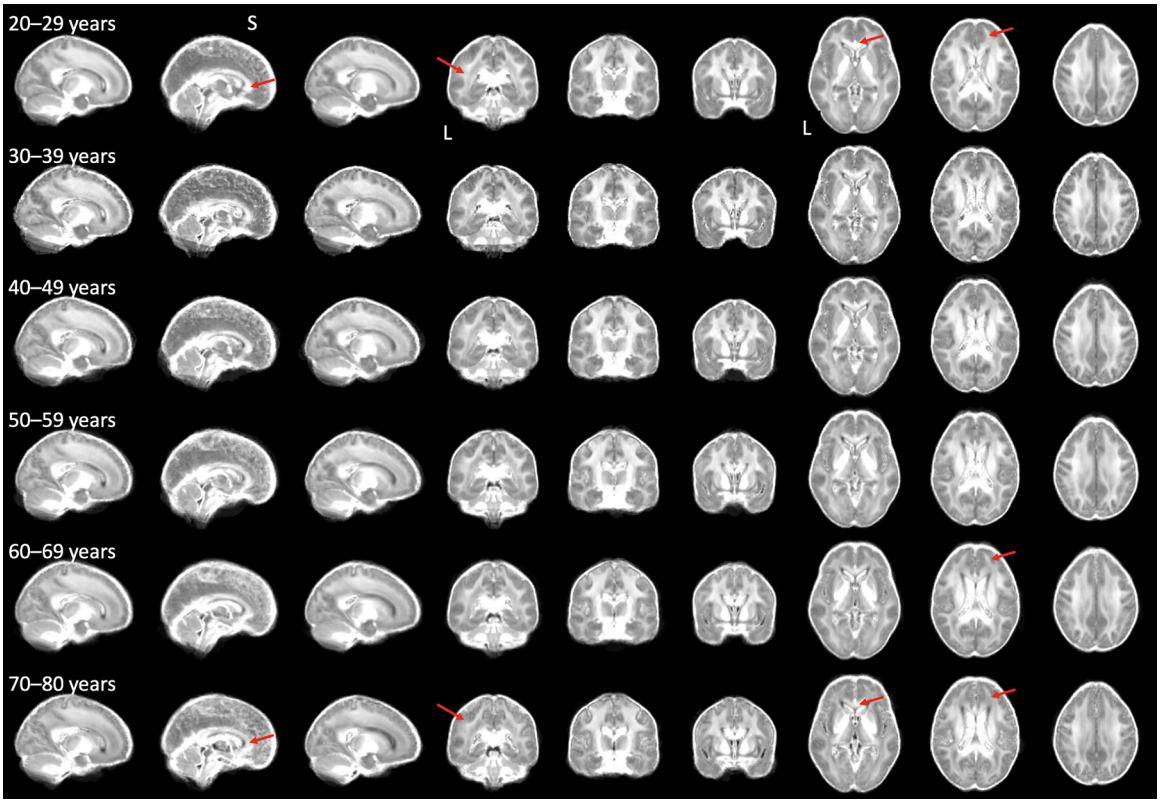

Fig. 2. Decade-averaged whole-brain maps of ICVF. The ICVF values were averaged across participants on maps co-registered in MNI space (see Methods), separately for each decade of life, for all participants involved in the analyses. Red arrows point to examples of age-related decrease in ICVF values (to be compared within each column). L: left, S: superior.

Table 3
Bivariate Pearson's correlations between intracranial volume and regional ICVF.

WM region	*r*	*p*	FDR-corrected *p*
Whole WM	0.27	0.010	0.035
Prefrontal	0.24	0.025	0.050
mPFC	0.25	0.017	0.048
EC	0.29	0.007	0.033
SLF	0.15	0.150	0.233
Genu CC	0.10	0.365	0.465
Body CC	0.12	0.269	0.377
Splenium CC	0.32	0.002	0.014
FX	0.29	0.007	0.033
TEMP	0.24	0.024	0.056
ALIC	0.09	0.403	0.470
UNC	0.34	0.001	0.014
CING	0.33	0.002	0.014
CST	0.23	0.028	0.049

Note: All correlations were on $N = 89$, bivariate, 2-tailed; see Table 1 for other abbreviations.

Table 4
Bivariate Pearson's correlations of ICVF with MWF.

WM region	*r*	*p*	FDR-corrected *p*
Whole WM	0.55	<0.001	<0.014
Prefrontal	0.59	<0.001	<0.014
mPFC	0.37	<0.001	<0.014
EC	0.34	0.001	0.007
SLF	0.64	<0.001	<0.014
Genu CC	0.60	<0.001	<0.014
Body CC	0.20	0.067	0.104
Splenium CC	0.30	0.005	0.018
FX	0.21	0.048	0.084
TEMP	0.21	0.047	0.094
ALIC	0.53	<0.001	<0.014
UNC	0.30	0.004	0.019
CING	0.26	0.014	0.033
CST	0.28	0.009	0.026

Note: All correlations were on $N = 89$, bivariate, 2-tailed; see *Table 1* for other abbreviations.

Axonal content: relations to metabolic syndrome and adiposity

Contrary to our prediction, there were no significant associations between regional ICVF and either MetS or adiposity scores, controlling for age, age^2, sex, race, ethnicity, income, and education. These results are presented in Appendix E.

Axonal content: associations with regional myelin

As shown in Table 4, ICVF and MWF were positively correlated in the majority of WM regions. The associations had large effect sizes in the SLF and genu CC, prefrontal and whole WM, and ALIC, medium effect sizes in the mPFC, EC, splenium CC, and UNC, and small effect sizes in the remaining regions (Fig. 3). Fig. 2-B shows averaged decade-representative whole-brain MWF maps.

Is the relationship between myelin and MetS/adiposity independent of axonal content?

Knowing that ICVF and MWF are related, we tested whether the previously observed negative associations between regional MWF and MetS or adiposity scores [26] are independent of regional ICVF. To this end, we first replicated the regression models for select regions using the current sample (see the grey row in Table 5). Next, we added regional ICVF to the model. Table 5 shows that the model fit improved after adding regional ICVF to explain variance in respective regional MWF.

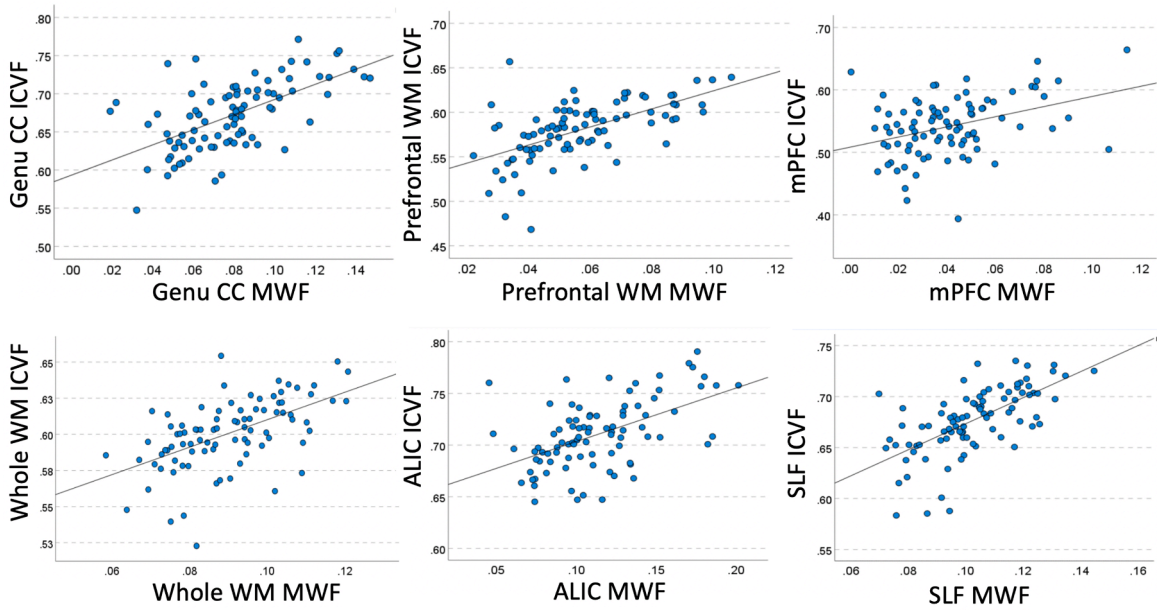

Fig. 3. Example bivariate region-specific correlations of MWF with ICVF. For abbreviations, see Table 1.

Table 5
Associations between regional MWF and either MetS risk score or adiposity sub-scores, controlling for age, age^2, sex, race, ethnicity, education, income, and regional ICVF.

DV	IV	Std. β	t	p	FDR-corrected p	ΔR^2	*Overall model fit* *Adjusted* R^2	p
UNC MWF	MetS	−0.47	−3.92	<0.001			0.17	0.003
	ICVF	0.27	2.18	.032			0.21	<0.001
	MetS	−0.45	−3.78	<0.001	<0.007	0.16 p<0.001		
Prefrontal MWF	MetS	−0.37	−3.00	0.004			0.15	0.006
	ICVF	0.63	6.00	<0.001			0.41	<0.001
	MetS	−0.33	−3.24	0.002	0.005	0.07 p = 0.002		
UNC MWF	Adiposity	−0.56	−5.19	<0.001			0.26	<0.001
	ICVF	0.22	1.85	0.069			0.28	<0.001
	Adiposity	−0.52	−4.89	<0.001	<0.007	0.20 p<0.001		
Genu CC MWF	Adiposity	−0.40	−3.82	<0.001			0.31	<0.001
	ICVF	0.45	4.12	<0.001			0.42	<0.001
	Adiposity	−0.32	−3.32	0.001	0.004	0.07 p = 0.001		
Prefrontal MWF	Adiposity	−0.46	−4.26	<0.001			0.23	<0.001
	ICVF	0.59	5.87	<0.001			0.46	<0.001
	Adiposity	−0.39	−4.28	<0.001	<0.007	0.11 p<0.001		
mPFC MWF	Adiposity	−0.40	−3.68	<0.001			0.23	<0.001
	ICVF	0.23	1.99	0.050			0.26	<0.001
	Adiposity	−0.36	−3.29	0.001	0.004	0.09 p = 0.001		
EC MWF	Adiposity	−0.36	−3.32	0.001			0.24	<0.001
	ICVF	0.41	3.94	<0.001			0.36	<0.001
	Adiposity	−0.29	−2.91	0.005	0.009	0.06 p = 0.005		

Note: DV: dependent variable of a modal. IV: independent variables, in addition to age (centered), age^2, sex, race, ethnicity, education, income. For each DV (regional MWF), the first line (marked in grey) is presented for comparison and is a replication of the results presented in [26] (n = 90) with the current sample size (n = 89). The remaining two lines present the regression results for the two IVs of interest: regional ICVF and MetS/Adiposity. Std. β: standardized beta coefficient. ΔR^2: R^2 change for MetS or adiposity scores in the final model.

Related to this, in all regions, ICVF explained a significant amount of variance in regional MWF. However, adding ICVF to the model did not affect the negative associations between MetS or adiposity and MWF.

Discussion

The current study investigated the age-, sex- and health-related differences in intra-axonal volume fraction in the white matter of cognitively and neurologically healthy adults. Our main findings are: 1) There were both linear and quadratic correlations of ICVF with age, with

distinct regional variability; 2) Men had greater ICVF than women, regardless of age, but this relationship was no longer present after accounting for intracranial volume; 3) ICVF was positively correlated with MWF in all examined WM regions; 4) Neither MetS risk score nor adiposity scores were related to ICVF; 5) The adiposity- or MetS-myelin associations were independent of regional ICVF.

Region-, age- and sex-related differences in axonal content

We observed the greatest ICVF in the WM regions containing the projection fibers (i.e., the corticospinal tract) or early-myelinating commissural fibers (body and splenium of corpus callosum) and the lowest in the late-myelinating association (e.g., uncinate) and prefrontal fibers (e.g., genu corpus callosum medial prefrontal WM). This is consistent with earlier histological studies on human WM [3,44–46].

Next, we observed a negative correlation of ICVF with age in all studied WM regions except the fornix and the corticospinal tract. The linear or quadratic negative correlations (in a region-dependent fashion) that are the strongest in frontal WM regions are consistent among studies involving middle-aged to older-adults (age ca. 45–80 years; [9,13,15–17]), as well as studies including the entire adult lifespan (ca. age 20–80; [8,10,12,18,19]). Some studies with smaller samples that weighted more heavily on participants representing early development to middle-age (ca. 7–60 years) reported increases in ICVF [20], mixed linear increases with quadratic increases [11], or no associations with age [14]. Together, our findings and those of others point to either linear negative or quadratic, inverted U-shaped associations of ICVF with age in most WM regions. These patterns indicate that axonal density or diameter (or both) follow the myelin maturation and deterioration trajectory, with the increase in both myelin and ICVF until the peak in middle age and subsequently decreasing in older age (also discussed in [12,18], and [26]). Our finding of a positive association of ICVF with age in the corticospinal tract is similar to a localized positive correlation in the cerebral peduncles [18] and could represent protracted increases in axonal volume in the early-myelinating regions, but warrants future investigation. Finally, the increase in ICVF with age in the fornix was earlier reported by Billiet et al. [11], however, others reported negative associations [19]. Given the possible contamination with CSF partial volume when studying fornix and the resulting errors in the NODDI model estimation, these inconsistencies need to be resolved with higher spatial resolution diffusion imaging.

To date, the limited number of studies investigating sex differences in ICVF have yielded mixed results. Three studies ([8,17], and [19]) reported no effects of sex on ICVF or the related axonal volume fraction [12] or age x sex interactions. Qian et al. [18] reported no age by sex interactions, but 2 to 6% higher ICVF values in women than men in the genu of corpus callosum, longitudinal fasciculus, and forceps minor (significant before FDR correction). An analysis of sex effects in a sample of 15,628 adults from the UK biobank study (45–80 years) showed only weak and scattered effects of sex on ICVF and age x sex interaction. Specifically, men had greater ICVF in the full WM, and women had greater ICVF in the corpus callosum but showed a steeper ICVF decline with age [15]. Taken together, our findings of no age x sex interactions on ICVF are consistent with the majority of previous reports. Our findings that ICVF was greater in men than women, but these differences were accounted for by the intracranial volume, suggests that future studies on WM microstructure should take into account anatomical differences between sexes. Given the uneven sex distribution, any sex differences in ICVF should be treated with caution.

Regional associations of myelin and axonal content estimates

Our results, which reveal predominantly medium to large effect size positive associations between ICVF and MWF, are consistent with the findings of Billiet et al. [11]. They observed a strong correlation between MWF and ICVF in the whole WM, estimated using the same methods as employed in the current study. Specifically, MWF and ICVF shared 33 % of variance in a sample of 59 healthy adults of age 17–70 years [11]. Similarly, De Santis et al. [21] observed a large effect size correlation (about 56 % shared variance) between axonal density (estimated as restricted fraction in the composite hindered and restricted model of diffusion) and MWF (estimated using mcDESPOT) in several tractography-defined tracts in a small sample of young adults. Results reported by Billiet et al. [11], De Santis et al. [21] and by us are of larger effect sizes than recently reported by Qian et al. [18], who observed positive associations between MWF and ICVF but predominantly of negligible to small effect size (0–6 % shared variance). The largest associations were reported in the occipital and temporal lobes, and genu of corpus callosum, with shared variance of only 9–12 % [18]. These discrepancies could be explained by differences in sample sizes ($n = 17$–59 in previous studies vs. $n = 89$ in the current study), different definitions of regions of interest (atlas-based or on WM skeleton), and different methods for MWF and ICVF estimation. Together, our results suggest that the MWF and ICVF are closely related, which is consistent with WM structure, physiology, and function. Yet, the association between axonal and myelin content may differ not only across the WM regions, but is possibly altered by age and disease processes, which needs to be determined in future longitudinal studies.

Selective vulnerability of myelin to MetS and adiposity, without involvement of axons

Contrary to our prediction, we found no evidence for an association between MetS or adiposity and ICVF. Furthermore, addition of ICVF to the model improved the overall prediction of MWF; however, it had no effect on the correlation with MetS or adiposity. Therefore, our results suggest that MetS and adiposity may be selectively related to myelin health. It is important to note that these findings may be true only for cognitively and neurologically healthy adults, which we recruited using strict exclusion criteria, also regarding other conditions that could affect WM health such as severe hypertension, hormonal imbalances, other medications, substance use, etc. It is very plausible that there would be an association between MetS and axonal content in a sample containing people with more advanced stages or a longer history of MetS. In other words, we hypothesize that MetS may first exert negative effects on myelin, followed by deterioration in axons at later disease stages, which needs to be tested in future longitudinal studies. Finally, ICVF derived from NODDI is not a direct measure of axonal content, but an estimate that is affected by several physiological, modeling, and experimental parameters (as discussed in the Limitations section). Therefore, the association of metabolic health and axonal content needs to be revisited using other MRI techniques and experimental designs (e.g., larger and more b-values), and larger cohort sizes.

Next, although our study is unable to determine the pathways linking MetS to myelin, several candidate mechanisms have been proposed, with cholesterol metabolism gaining more attention recently [47]. Cholesterol plays a key role in regulation of myelin biosynthesis and deterioration [48,49] and aberrant cholesterol deposition coincides with reduced myelination in the brains of APOE4 carrier mice, whereas pharmacological facilitation of its transport can recover myelination [50]. In addition, some of cholesterol forms such as the 27-hydroxycholesterol are transported across the blood-brain barrier, are toxic to immature oligodendrocytes, and alter myelin composition [51]. Thus, our results suggest that myelin health may be a candidate link between MetS and cognitive decline, yet the metabolic mechanisms, which could be targeted by lipid-based therapy and dietary interventions, remain to be identified.

Limitations

The main limitation of this study is the use of the NODDI model, which, although more sophisticated than diffusion tensor imaging,

provides only an estimate of ICVF, not a true measurement of intra-axonal volume. For example, NODDI is known to overestimate the isotropically diffusion water fraction and to provide unrealistically high ICVF values in WM which estimates are dependent on echo time [8,52,7]. For example, our ICVF values ranged 53–74 %, consistent with the ICVF results from the original NODDI model, and greater than the ICVF values obtained with the constrained NODDI [8]. Thus, future studies need to replicate the current findings using alternative or improved diffusion models.

In addition, there are several limitations such as the binary self-reported status of a history of dyslipidemia and hyperglycemia as components of the MetS score, which may be inaccurate and do not reflect a range of fasting blood glucose, cholesterol and triglyceride levels [26]. Also, despite strict inclusion and exclusion criteria and the use of TBSS to align and skeletonize MWF values in the center of WM tracts, we cannot exclude that both ICVF and MWF values may be to some extent affected by macrostructural changes related to aging and MetS individual components, such as global brain tissue atrophy and WM hyperintensities [47,53]. Finally, women are overrepresented in our sample, which is a common challenge in aging studies including strict inclusion/exclusion criteria. Uneven sex distribution calls for the sex differences in ICVF to be treated with caution.

Conclusions

The current study shows that in neurologically, cognitively, and physically healthy adults, the estimates of axonal content declines with age, positively correlates with myelin, and is lower in women than men, but this difference was accounted for by the intracranial volume. Furthermore, our data suggests that MetS risk is associated with lower myelin content but not a decreased estimate of axonal content. Our results encourage revisiting the current findings with other MRI techniques to estimate axonal content or integrity, as well as further research into the physiological mechanisms linking peripheral metabolism with myelin's health. Understanding these mechanisms could lead to the development of new therapies, diet, and exercise interventions protecting myelin health. Those approaches may help decelerate brain aging and support existing treatments against AD. In addition, future longitudinal studies should assess whether disruption of axonal content is present in patients with the more advanced stages of MetS or chronic obesity.

Data statement

The data used to generate the results presented in this work is available upon request from the corresponding author, due to the ongoing data collection.

CRediT authorship contribution statement

Agnieszka Z Burzynska: Writing – review & editing, Writing – original draft, Visualization, Supervision, Software, Resources, Project administration, Methodology, Investigation, Funding acquisition, Formal analysis, Data curation. **Charles Anderson:** Writing – review & editing, Software, Methodology, Funding acquisition. **David B. Arciniegas:** Writing – review & editing, Resources, Investigation, Funding acquisition. **Vince Calhoun:** Writing – review & editing, Software, Resources, Methodology, Funding acquisition. **In-Young Choi:** Writing – review & editing, Software, Resources, Methodology, Funding acquisition, Conceptualization. **Andrea Mendez Colmenares:** Writing – review & editing, Methodology, Investigation, Data curation. **Arthur F Kramer:** Writing – review & editing, Resources, Funding acquisition, Conceptualization. **Kaigang Li:** Writing – review & editing, Methodology, Funding acquisition, Data curation. **Jongho Lee:** Writing – review & editing, Validation, Software, Resources, Methodology, Investigation, Funding acquisition, Conceptualization. **Phil Lee:** Writing – review & editing, Software, Resources, Methodology, Investigation, Funding acquisition, Conceptualization. **Michael L Thomas:** Writing – review & editing, Methodology, Funding acquisition.

Declaration of competing interest

None.

Acknowledgements

The study was supported by AARG-NTF-21–849265 from the Alzheimer's Association and 1R21AG068939–01A1 from the National Institutes on Aging to AZ Burzynska.

We thank the current and past members of the BRAiN lab for their help in data collection: Grace Hiner, Samantha Umland, Jake Lonergan, Raghuram Kakinada, Neveah Newton, Miles Hopkins, Nick Stirbis, Brandon Paez, and Tess Armstrong. We thank Vineet Agarwal for being the study data wizard. We thank all of your participants who volunteered for the study and Kelly Lyell for help with recruitment. We thank Joon Yul Choi for his help in GRASE image processing.

Supplementary materials

Supplementary material associated with this article can be found, in the online version, at doi:10.1016/j.cccb.2024.100203.

References

[1] C.H. van Dyck, C.J. Swanson, P. Aisen, R.J. Bateman, C. Chen, M. Gee, M. Kanekiyo, D. Li, L. Reyderman, S. Cohen, L. Froelich, S. Katayama, M. Sabbagh, B. Vellas, D. Watson, S. Dhadda, M. Irizarry, L.D. Kramer, T. Iwatsubo, Lecanemab in Early Alzheimer's Disease, N. Engl. J. Med. 388 (1) (2023) 9–21, https://doi.org/10.1056/NEJMoa2212948.

[2] G. Bartzokis, Age-related myelin breakdown: a developmental model of cognitive decline and Alzheimer's disease, Neurobiol. Aging 25 (1) (2004) 5–18. http://www.ncbi.nlm.nih.gov/pubmed/14675724.

[3] G. Bartzokis, Alzheimer's disease as homeostatic responses to age-related myelin breakdown, Neurobiol. Aging 32 (2011) 1341–1371, https://doi.org/10.1016/j.neurobiolaging.2009.08.007.

[4] S.E. Nasrabady, B. Rizvi, J.E. Goldman, A.M. Brickman, White matter changes in Alzheimer's disease: a focus on myelin and oligodendrocytes, Acta Neuropathol. Commun. 6 (1) (2018) 22, https://doi.org/10.1186/s40478-018-0515-3.

[5] D.K. Jones, T.R. Knösche, R. Turner, White matter integrity, fiber count, and other fallacies: the do's and don'ts of diffusion MRI, Neuroimage 73 (2013) 239–254, https://doi.org/10.1016/j.neuroimage.2012.06.081.

[6] Denis Le Bihan, Molecular diffusion, tissue microdynamics and microstructure, NMR Biomed. 8 (1995) 375–386.

[7] H. Zhang, T. Schneider, C.A. Wheeler-Kingshott, D.C. Alexander, NODDI: practical in vivo neurite orientation dispersion and density imaging of the human brain, Neuroimage 61 (4) (2012) 1000–1016, https://doi.org/10.1016/J.NEUROIMAGE.2012.03.072.

[8] M.H. Alsameen, Z. Gong, W. Qian, M. Kiely, C. Triebswetter, C.M. Bergeron, L. E. Cortina, M.E. Faulkner, J.P. Laporte, M. Bouhrara, C-NODDI: a constrained NODDI model for axonal density and orientation determinations in cerebral white matter, Front. Neurol. 14 (2023) 1205426, https://doi.org/10.3389/fneur.2023.1205426.

[9] C.E. Bauer, V. Zachariou, P. Maillard, A. Caprihan, B.T Gold, Multi-compartment diffusion magnetic resonance imaging models link tract-related characteristics with working memory performance in healthy older adults, Front. Aging Neurosci. 5 (14) (2022) 995425, https://doi.org/10.3389/fnagi.2022.995425.

[10] D. Beck, A.G. de Lange, I.I. Maximov, G. Richard, O.A. Andreassen, J.E. Nordvik, L. T. Westlye, White matter microstructure across the adult lifespan: a mixed longitudinal and cross-sectional study using advanced diffusion models and brain-age prediction, Neuroimage 224 (2021) 117441, https://doi.org/10.1016/j.neuroimage.2020.117441.

[11] T. Billiet, M. Vandenbulcke, B. Mädler, R. Peeters, T. Dhollander, H. Zhang, S. Deprez, B.R. Van den Bergh, S. Sunaert, L. Emsell, Age-related microstructural differences quantified using myelin water imaging and advanced diffusion MRI, Neurobiol. Aging 36 (6) (2015) 2107–2121, https://doi.org/10.1016/j.neurobiolaging.2015.02.029.

[12] M. Bouhrara, N. Khattar, P. Elango, S.M. Resnick, L. Ferrucci, R.G. Spencer, Evidence of association between obesity and lower cerebral myelin content in cognitively unimpaired adults, Int. J. Obes. 45 (4) (2021) 850–859, https://doi.org/10.1038/s41366-021-00749-x.

[13] S.R. Cox, S.J. Ritchie, E.M. Tucker-Drob, D.C. Liewald, S.P. Hagenaars, G. Davies, J.M. Wardlaw, C.R. Gale, M.E. Bastin, I.J. Deary, Ageing and brain white matter

structure in 3,513 UK Biobank participants, Nat. Commun. 7 (2016) 13629, https://doi.org/10.1038/ncomms13629.
[14] C. Kodiweera, A.L. Alexander, J. Harezlak, T.W. McAllister, Y.C. Wu, Age effects and sex differences in human brain white matter of young to middle-aged adults: a DTI, NODDI, and q-space study, Neuroimage 128 (2016) 180–192, https://doi.org/10.1016/j.neuroimage.2015.12.033.
[15] K.E. Lawrence, L. Nabulsi, V. Santhalingam, Z. Abaryan, J.E. Villalon-Reina, T. M. Nir, I. Ba Gari, A.H. Zhu, E. Haddad, A.M. Muir, E. Laltoo, N. Jahanshad, P. M Thompson, Age and sex effects on advanced white matter microstructure measures in 15,628 older adults: a UK biobank study, Brain ImAging Behav. 15 (6) (2021) 2813–2823, https://doi.org/10.1007/s11682-021-00548-y.
[16] A.P. Merluzzi, D.C. Dean 3rd, N. Adluru, G.S. Suryawanshi, O.C. Okonkwo, J. M. Oh, B.P. Hermann, M.A. Sager, S. Asthana, H. Zhang, S.C. Johnson, A. L. Alexander, B.B. Bendlin, Age-dependent differences in brain tissue microstructure assessed with neurite orientation dispersion and density imaging, Neurobiol. Aging 43 (2016) 79–88, https://doi.org/10.1016/j.neurobiolaging.2016.03.026.
[17] A. Motovylyak, N.M. Vogt, N. Adluru, Y. Ma, R. Wang, J.M. Oh, S.R. Kecskemeti, A. L. Alexander, D.C. Dean, C.L. Gallagher, M.A. Sager, B.P. Hermann, H.A. Rowley, S. C. Johnson, S. Asthana, B.B. Bendlin, O.C. Okonkwo, Age-related differences in white matter microstructure measured by advanced diffusion MRI in healthy older adults at risk for Alzheimer's disease, Aging Brain 2 (2022) 100030, https://doi.org/10.1016/j.nbas.2022.100030.
[18] W. Qian, N. Khattar, L.E. Cortina, R.G. Spencer, M. Bouhrara, Nonlinear associations of neurite density and myelin content with age revealed using multicomponent diffusion and relaxometry magnetic resonance imaging, Neuroimage 223 (2020) 117369, https://doi.org/10.1016/j.neuroimage.2020.117369.
[19] S. Raghavan, R.I. Reid, S.A. Przybelski, T.G. Lesnick, J. Graff-Radford, C. G. Schwarz, D.S. Knopman, M.M. Mielke, M.M. Machulda, R.C. Petersen, C. R. Jack Jr, P Vemuri, Diffusion models reveal white matter microstructural changes with ageing, pathology and cognition, Brain Commun. 3 (2) (2021) fcab106, https://doi.org/10.1093/braincomms/fcab106.
[20] Y.S. Chang, J.P. Owen, N.J. Pojman, T. Thieu, P. Bukshpun, M.L. Wakahiro, J. I. Berman, T.P. Roberts, S.S. Nagarajan, E.H. Sherr, P. Mukherjee, White matter changes of neurite density and fiber orientation dispersion during human brain maturation, PloS One 10 (6) (2015) e0123656, https://doi.org/10.1371/journal.pone.0123656.
[21] S. De Santis, M. Drakesmith, S. Bells, Y. Assaf, D.K. Jones, Why diffusion tensor MRI does well only some of the time: variance and covariance of white matter tissue microstructure attributes in the living human brain, Neuroimage 89 (100) (2014) 35–44, https://doi.org/10.1016/j.neuroimage.2013.12.003. Epub 2013 Dec 14. PMID: 24342225; PMCID: PMC3988851.
[22] R.B. Ervin, Prevalence of metabolic syndrome among adults 20 years of age and over, by sex, age, race and ethnicity, and body mass index: united States, 2003-2006, Natl. Health Stat. Report. (2009) 13.
[23] H.M. Lakka, D.E. Laaksonen, T.A. Lakka, L.K. Niskanen, E. Kumpusalo, J. Tuomilehto, J.T. Salonen, The metabolic syndrome and total and cardiovascular disease mortality in middle-aged men, J. Am. Med. Assoc. 288 (21) (2002), https://doi.org/10.1001/jama.288.21.2709.
[24] K.G.M.M. Alberti, P. Zimmet, J. Shaw, Metabolic syndrome - A new world-wide definition. A consensus statement from the International Diabetes Federation, in: Diabetic Medicine, 23, 2006, https://doi.org/10.1111/j.1464-5491.2006.01858.x. Issue 5.
[25] S. Kullmann, M.F. Callaghan, M. Heni, N. Weiskopf, K. Scheffler, H.U. Häring, A. Fritsche, R. Veit, H. Preissl, Specific white matter tissue microstructure changes associated with obesity, Neuroimage 125 (2016) 36–44, https://doi.org/10.1016/j.neuroimage.2015.10.006.
[26] A.Z. Burzynska, C. Anderson, D.B. Arciniegas, V. Calhoun, I.-Y. Choi, A. Mendez Colmenares, G. Hiner, A.F. Kramer, K. Li, J. Lee, P. Lee, S.H. Oh, S. Umland, M. L. Thomas, Metabolic syndrome and adiposity: risk factors for decreased myelin in cognitively healthy adults, Cereb. Circ. Cogn. Behav. 5 (2023) 100180, https://doi.org/10.1016/j.cccb.2023.100180.
[27] M. Simons, K.A. Nave, Oligodendrocytes: myelination and axonal support, in: Cold Spring Harbor Perspectives in Biology, 8, 2016, https://doi.org/10.1101/cshperspect.a020479. Issue 1.
[28] S.Y. Bookheimer, D.H. Salat, M. Terpstra, B.M. Ances, D.M. Barch, R.L. Buckner, G. C. Burgess, S.W. Curtiss, M. Diaz-Santos, J.S. Elam, B. Fischl, D.N. Greve, H. A. Hagy, M.P. Harms, O.M. Hatch, T. Hedden, C. Hodge, K.C. Japardi, T.P. Kuhn, E. Yacoub, The Lifespan Human Connectome Project in Aging: an overview, Neuroimage 185 (2019) 335–348, https://doi.org/10.1016/j.neuroimage.2018.10.009.
[29] C.A. de Jager, M.M. Budge, R. Clarke, Utility of TICS-M for the assessment of cognitive function in older adults, Int. J. Geriatr. Psychiatry 18 (4) (2003) 318–324, https://doi.org/10.1002/gps.830.
[30] R.M. Crum, J.C. Anthony, S.S. Bassett, M.F. Folstein, Population-Based Norms for the Mini-Mental State Examination by Age and Educational Level, JAMA: The Journal of the American Medical Association 269 (18) (1993) 2386–2391, https://doi.org/10.1001/jama.1993.03500180078038.
[31] B.W. Rovner, M.F. Folstein, Mini-mental state exam in clinical practice, Hosp. Pract. 22 (1A) (1987) 99, 103, 106, 110, http://www.ncbi.nlm.nih.gov/pubmed/3100557.
[32] J.C. Morris, The clinical dementia rating (CDR): current version and scoring rules, Neurology. 43 (1993) 2412, https://doi.org/10.1212/wnl.43.11.2412-a.
[33] J.A. Yasavage, J.I. Sheikh, Geriatric Depression Scale (GDS): recent Evidence and Development of a Shorter Version, Clin. Gerontol. 5 (1–2) (1986) 165–173.
[34] I.M. Nasrallah, N.M. Pajewski, A.P. Auchus, G. Chelune, A.K. Cheung, M. L. Cleveland, L.H. Coker, M.G. Crowe, W.C. Cushman, J.A. Cutler, C. Davatzikos, L. Desiderio, J. Doshi, G. Erus, L.J. Fine, S.A. Gaussoin, D. Harris, K.C. Johnson, P. L. Kimmel, R.N. Bryan, Association of intensive vs standard blood pressure control with cerebral white matter lesions, JAMA - Journal of the American Medical Association 322 (6) (2019) 524–534, https://doi.org/10.1001/jama.2019.10551.
[35] N. Medic, P. Kochunov, H. Ziauddeen, K.D. Ersche, P.J. Nathan, L. Ronan, P. C. Fletcher, BMI-related cortical morphometry changes are associated with altered white matter structure, Int. J. Obes. 43 (3) (2019) 1, https://doi.org/10.1038/s41366-018-0269-9.
[36] J.E. Winter, R.J. MacInnis, N. Wattanapenpaiboon, C.A. Nowson, BMI and all-cause mortality in older adults: a meta-analysis, American Journal of Clinical Nutrition 99 (4) (2014) 875–890, https://doi.org/10.3945/ajcn.113.068122.
[37] W.G. Rosen, R.D. Terry, P.A. Fuld, R. Katzman, A. Peck, Pathological verification of ischemic score in differentiation of dementias, Ann. Neurol. 7 (5) (1980) 486–488, https://doi.org/10.1002/ana.410070516.
[38] J.L.R. Andersson, S. Skare, J. Ashburner, How to correct susceptibility distortions in spin-echo echo-planar images: application to diffusion tensor imaging, Neuroimage 20 (2) (2003) 870–888, https://doi.org/10.1016/S1053-8119(03)00336-7.
[39] S.M. Smith, M. Jenkinson, M.W. Woolrich, C.F. Beckmann, T.E.J. Behrens, H. Johansen-Berg, P.R. Bannister, M. De Luca, I. Drobnjak, D.E. Flitney, R.K. Niazy, J. Saunders, J. Vickers, Y. Zhang, N. De Stefano, J.M. Brady, P.M. Matthews, Advances in functional and structural MR image analysis and implementation as FSL, Neuroimage 23 (Suppl 1) (2004) S208–S219, https://doi.org/10.1016/j.neuroimage.2004.07.051.
[40] J.L.R. Andersson, S.N. Sotiropoulos, An integrated approach to correction for off-resonance effects and subject movement in diffusion MR imaging, Neuroimage 125 (2016), https://doi.org/10.1016/j.neuroimage.2015.10.019.
[41] S.M. Smith, H. Johansen-Berg, M. Jenkinson, D. Rueckert, T.E. Nichols, K.L. Miller, M.D. Robson, D.K. Jones, J.C. Klein, A.J. Bartsch, T.E.J. Behrens, Acquisition and voxelwise analysis of multi-subject diffusion data with tract-based spatial statistics, Nat. Protoc. 2 (3) (2007) 499–503. http://www.ncbi.nlm.nih.gov/pubmed/17406613.
[42] T.D. Verstynen, A. Weinstein, K.I. Erickson, L.K. Sheu, A.L. Marsland, P. J. Gianaros, Competing physiological pathways link individual differences in weight and abdominal adiposity to white matter microstructure, Neuroimage 79 (2013) 129–137, https://doi.org/10.1016/j.neuroimage.2013.04.075.
[43] J. Cohen, Statistical Power Analysis For the Behavioral Sciences, 2nd ed., Erlbaum, Hillsdale, MI, USA, 1988. ISBN 0-8058-0283-5.
[44] F. Aboitiz, A.B. Scheibel, R.S. Fisher, E. Zaidel, Fiber composition of the human corpus callosum, Brain Res. 598 (1–2) (1992) 143–153. http://www.ncbi.nlm.nih.gov/pubmed/1486477.
[45] P.J. Armati, E.K. Mathey, The biology of oligodendrocytes. The Biology of Oligodendrocytes, 2010, https://doi.org/10.1017/CBO9780511782121.
[46] L. Marner, J.R. Nyengaard, Y. Tang, B. Pakkenberg, Marked loss of myelinated nerve fibers in the human brain with age, Journal of Comparative Neurology 462 (2) (2003) 144–152, https://doi.org/10.1002/cne.10714.
[47] F.J. Alfaro, A. Gavrieli, P. Saade-Lemus, V.A. Lioutas, J. Upadhyay, V. Novak, White matter microstructure and cognitive decline in metabolic syndrome: a review of diffusion tensor imaging, in: Metabolism: Clinical and Experimental, Vol. 78, 2018, https://doi.org/10.1016/j.metabol.2017.08.009.
[48] S.A. Berghoff, L. Spieth, G. Saher, Local cholesterol metabolism orchestrates remyelination, Trends Neurosci. 45 (4) (2022) 272–283, https://doi.org/10.1016/j.tins.2022.01.001.
[49] G. Saher, S. Quintes, K.A. Nave, Cholesterol: a novel regulatory role in myelin formation, The Neuroscientist: a review journal bringing neurobiology, neurology and psychiatry 17 (1) (2011) 79–93, https://doi.org/10.1177/1073858410373835.
[50] J.W. Blanchard, L.A. Akay, J. Davila-Velderrain, D. von Maydell, H. Mathys, S. M. Davidson, A. Effenberger, C.Y. Chen, K. Maner-Smith, I. Hajjar, E.A. Ortlund, M. Bula, E. Agbas, A. Ng, X. Jiang, M. Kahn, C. Blanco-Duque, N. Lavoie, L. Liu, R. Reyes, L.H. Tsai, APOE4 impairs myelination via cholesterol dysregulation in oligodendrocytes, Nature 611 (7937) (2022) 769–779, https://doi.org/10.1038/s41586-022-05439-w.
[51] V. Alanko, A. Gaminde-Blasco, T. Quintela-López, R. Loera-Valencia, A. Solomon, I. Björkhem, A. Cedazo-Minguez, S. Maioli, G. Tabacaru, M. Latorre-Leal, C. Matute, M. Kivipelto, E. Alberdi, A. Sandebring-Matton, 27-hydroxycholesterol promotes oligodendrocyte maturation: implications for hypercholesterolemia-associated brain white matter changes, Glia 71 (6) (2023) 1414–1428, https://doi.org/10.1002/glia.24348.
[52] T. Gong, Q. Tong, H. He, Y. Sun, J. Zhong, H. Zhang, MTE-NODDI: multi-TE NODDI for disentangling non-T2-weighted signal fractions from compartment-specific T2 relaxation times, Neuroimage 217 (2020) 116906, https://doi.org/10.1016/j.neuroimage.2020.116906.
[53] K.F. Yates, V. Sweat, P.L. Yau, M.M. Turchiano, A. Convit, Impact of Metabolic Syndrome on Cognition and Brain, Arterioscler. Thromb. Vasc. Biol. (9) (2012) 32, https://doi.org/10.1161/atvbaha.112.252759.